Condensate fluctuation and thermodynamics of mesoscopic Bose-Einstein condensates: A correlated many-body approach

Satadal Bhattacharyya[1] and Barnali Chakrabarti[2]
[1]*Department of Physics, Scottish Church College, 1 & 3 Urquhart Square, Kolkata 700 006, India*
[2]*Department of Physics, Presidency University, 86/1 College Street, Kolkata 700 073, India*
(Received 5 June 2015; revised manuscript received 15 September 2015; published 23 February 2016)

We present a correlated many-body approach to calculate the distribution function and fluctuations for a Bose-Einstein condensate with N interacting atoms in the harmonic confinement. The present formulation uses the recursion relation for the canonical ensemble partition function (Z). Z is calculated from the energy spectrum of the many-body effective potential, which keeps all possible two-body correlations and uses the realistic interatomic interaction. The condensate statistics are in very good agreement with earlier results of an ideal gas for which exact statistical moments for all temperature are known. We also present the numerical results of condensate statistics for real experimental situations. The calculated moments nicely exhibit the mesoscopic effect for a few hundred atoms, whereas the sharp fall in the variance for the large condensate near the critical temperature shows the possibility of phase transition. We also calculate the critical temperature for the mesoscopic regime. Our present calculation mimics the JILA experiment with ^{87}Rb atoms.

DOI: 10.1103/PhysRevA.93.023636

I. INTRODUCTION

Statistical properties of quantum many-body systems are the subject of great interest in statistical physics since long time back. Recently statistics of weakly interacting Bose gas have received attention due to the experimental realization of Bose-Einstein condensate (BEC) in ultracold trapped gases [1–5]. The total number of atoms in the condensate is strictly conserved, and the experiments on trapped BEC often consist of as few as a hundred atoms, which makes the system mesoscopic. For such systems, the grand-canonical description is not appropriate and it cannot describe the condensate fluctuation even qualitatively. The use of a grand-canonical approach yields the grand-canonical catastrophe [6], and the use of a canonical ensemble to calculate the fluctuation of such a mesoscopic system is mathematically complicated.

As for the ideal Bose gas (IG), the exact canonical recursion relation for the partition function is known, and the condensate statistics of IG is clearly understood [7–9]. Condensate statistics and thermodynamics of weakly interacting Bose gas (WIG) has also been extensively studied in canonical ensemble [10–18]. Most of the studies use the Bogoliubov approximation, however none of them are very accurate. Near the critical temperature T_c, the problem of interacting Bose gas becomes a difficult one and the correlation becomes substantial. Later the canonical recursion relation technique was substantially improved, considering the recursion is made over the number of states and excitations [13]. Although this technique gives a relatively good result for a very large number of particles, it is not so accurate near the critical temperature. In another series of similar work, the canonical ensemble recursion relation for the partition function of WIG is obtained by utilizing the canonical ensemble quasiparticle formalism, and condensate statistics of mesoscopic WIG BEC is discussed [14]. This work considers N particles in a cubical box and the temperature dependence of various statistical moments of condensate fluctuation are investigated.

However, the real experimental situation considers N interacting atoms in external harmonic confinement, and we do not find any systematic and thorough calculation which considers the real experimental situation and discusses several issues in the region $T \simeq T_c$. Thus the atom statistics of the mesoscopic BEC is still challenging and it is possible to measure experimentally in the near future. Until now only the statistics of the total number of atoms in the condensate have been measured experimentally. The BEC is often referred to as an atom laser, although the statistical properties of thermal equilibrium atoms are notably different than those of photons. The analogy between BEC and the laser threshold master equation approach has been described earlier [15], and the experimental technique of scattering of laser pulses from the quantum gas is proposed in Refs. [19–22] but not realized experimentally; however, it is possible to measure experimentally. Thus the calculation of condensate fluctuation for the real experimental situation with N interacting atoms in the harmonic confinement needs thorough investigation. In the present paper, we provide an *ab initio* but approximate many-body approach to calculate the probability of a distribution function N of atom condensate using the canonical partition function. We propose here the use of a two-body correlated basis function (TBCBF) and also choose the realistic interatomic interaction. The TBCBF is ideally suited for the dilute BEC, where three- and higher-body correlations are ignored. In our earlier works, we extensively used the TBCBF to discuss several static and dynamic properties of the condensate [23–25]. The TBCBF is basically a subset of the full hyperspherical harmonics (HH) which keeps all the basic features of the condensate, but it also greatly reduces the computational difficulty even for larger numbers of bosons. For our present study we chose ^{87}Rb atoms trapped in a spherically symmetric harmonic oscillator potential. The number of interacting atoms in the trap varies from as few as 50 to as high as 10 000. It allows us to study the mesoscopic region very carefully and also to observe how the different statistical fluctuations change with gradual increase in interatomic interaction. We first calculate the whole energy spectrum of the condensate and then calculate the canonical partition function using recursive

approaches [19,26]. Then all statistical fluctuations and the condensate statistics are calculated for the entire range of temperature.

The paper is organized as follows. Section II deals with the many-body formalism. Section III contains the calculation of various fluctuation quantities both for the ideal and interacting Bose gas under harmonic confinement. We also present thermodynamics for the mesoscopic BEC. Section IV concludes with a summary.

II. FORMALISM: CORRELATED POTENTIAL HARMONICS EXPANSION TECHNIQUE

Since the technique of the correlated potential harmonics expansion (CPHE) method adopted for the approximate solution of the many-body Schrödinger equation for the dilute Bose condensates is well established and documented [23–25], only a brief outline is presented below.

Consider a system of N identical bosons, each of mass m, confined in a spherically symmetric harmonic oscillator potential of frequency ω. The center-of-mass motion can be decoupled and the Schrödinger equation for the relative motion of the system is described by $N' = N - 1$ Jacobi vectors defined as

$$\vec{\zeta}_i = \sqrt{\frac{2i}{i+1}}\left(\vec{x}_{i+1} - \frac{1}{i}\sum_{j=1}^{i}\vec{x}_j\right), \quad (i = 1,...,N'), \tag{1}$$

where $\vec{x}_i$ is the position vector of the ith particle. The Schrödinger equation for the relative motion is

$$\left[-\frac{\hbar^2}{m}\sum_{i=1}^{N'}\nabla^2_{\vec{\zeta}_i} + V_{\rm trap}(\vec{\zeta}_1,...,\vec{\zeta}_{N'}) - E_R\right] \times \psi(\vec{\zeta}_1,...,\vec{\zeta}_{N'}) = 0. \tag{2}$$

Here the trapping potential ($V_{\rm trap} = \sum_{i=1}^{N}\frac{1}{2}m\omega^2 x_i^2$) and the net interatomic interaction [$V = \sum_{i,j<i}^{N} V(\vec{x}_i - \vec{x}_j)$] are expressed in terms of the Jacobi vectors. The energy of the relative motion is E_R. The evolution of the system can be viewed by following the motion of one point in $3N$-dimensional hyperspace. The polar coordinates of this point are expressed by the hyperspherical variables. A hyperradius is defined as

$$r = \left[\sum_{i=1}^{N'}\zeta_i^2\right]^{\frac{1}{2}}. \tag{3}$$

Remaining $(3N' - 1)$ variables are taken as the polar angles of N' Jacobi vectors and $N' - 1$ angles defining the relative lengths of these Jacobi vectors. These are collectively referred to as "hyperangles" [27]. The hyperspherical harmonics expansion method (HHEM) consists of expanding the relative wave function ψ in the complete set of hyperspherical harmonics (HH). Actually, the HH are the eigenfunctions of the grand orbital operator [hyperangular part of the N'-dimensional Laplace operator, given by the summation in the first term of Eq. (2)] [27]. Substitution of this expansion in Eq. (2) and projection on a particular HH give rise to a set of coupled differential equations (CDEs). This straightforward procedure becomes more and more difficult as A increases beyond 3, due to the very rapid increase in the degeneracy of the HH basis [27] for a given hyperorbital quantum number (K). The calculation of potential matrix elements also becomes increasingly difficult and tedious as N increases. Even though this transparent procedure takes care of *all many-body correlations*, a full calculation by the HHEM becomes difficult for $N > 3$. However, in a recent work [28] up to $N = 6$ particles have been considered in the calculation of the universality and scaling in the N-body Efimov physics.

The density of a typical Bose-Einstein condensate is very low so that the average interparticle distance is much larger than the range of interatomic interactions and the three-body collisions are completely negligible. We may also neglect any correlations higher than two-body correlations in such an extremely dilute system. Then the expansion basis for the many-body wave function can be restricted to the subset of HH, which involves two-body correlations only. This drastically reduces the algebraic and numerical complexity of the problem. Under this condition, ψ can be decomposed in Faddeev components ψ_{ij} for the (ij)-interacting pair, whose separation is $\vec{r}_{ij}$ [29]:

$$\psi = \sum_{i,j>i}^{N}\psi_{ij}(\vec{r}_{ij},r). \tag{4}$$

The Faddeev component ψ_{ij} describes the motion of the system when the ij pair interacts while the remaining $N - 2$ are essentially spectators. Clearly, then, $\psi_{ij}(\vec{r}_{ij},r)$ can be expanded in a subset of HH, called the potential harmonics (PH), which is sufficient for the expansion of the interaction potential $V(\vec{r}_{ij})$ as a function in the hyperangular space. A simple analytic expression for the potential harmonic $\mathcal{P}^{lm}_{2K+l}(\Omega^{ij}_{N'})$ is possible and may be found in [29]. Here, l and m are the orbital angular momentum of the system and its projection and K is the $3N'$-dimensional grand orbital quantum number. Expansion of the Faddeev component in the PH basis is given as

$$\psi_{ij}(\vec{r}_{ij},r) = r^{-\frac{(3N-1)}{2}}\sum_{K}\mathcal{P}^{lm}_{2K+l}\left(\Omega^{ij}_{N'}\right)u^l_K(r). \tag{5}$$

Then Eq. (2) can now be written as

$$(T + V_{\rm trap} - E_R)\psi_{ij} = -V(r_{ij})\sum_{k,l>k}^{N}\psi_{kl}, \tag{6}$$

where T represents the total kinetic energy. Due to the strong short-range repulsion of the interatomic interaction, ψ_{ij} must be very small for small r_{ij}. However, the leading terms of PH corresponding to small values of the grand orbital quantum number K do not have this behavior. Hence the rate of convergence is very slow. The convergence rate is improved greatly by including an additional short-range correlation function $\eta(\vec{r}_{ij})$, which is chosen to be the zero-energy solution of the two-body Schrödinger equation,

$$-\frac{\hbar^2}{m}\frac{1}{r_{ij}^2}\frac{d}{dr_{ij}}\left(r_{ij}^2\frac{d\eta(r_{ij})}{dr_{ij}}\right) + V(r_{ij})\eta(r_{ij}) = 0, \tag{7}$$

and hence has the same short-range behavior as $\psi_{ij}(\vec{r}_{ij},r)$.

In a typical BEC achieved in laboratories, the average interparticle separation is much larger than the range of two-body interaction. Under this condition, the two-body interaction can be represented by the s-wave scattering length (a_s). The asymptotic form of $\eta(\vec{r}_{ij})$ reflects this, as it is given by $C(1-\frac{a_s}{r_{ij}})$ for large r_{ij} [30]. In our calculation we choose the interatomic potential $V(\vec{r}_{ij})$ to be the van der Waals potential whose short-range repulsion is modeled by a hard core of radius r_c:

$$V(\vec{r}_{ij}) = \infty \quad \text{for} \quad r < r_c$$
$$= -\frac{C_6}{{r_{ij}}^6} \quad \text{for} \quad r_{ij} \geqslant r_c. \tag{8}$$

The value of r_c is adjusted to reproduce desired a_s in the asymptotic form of $\eta(\vec{r}_{ij})$ [30]. This ensures that the correct effective two-body interaction, expressed in terms of a_s, appropriate for the condensate has been taken.

Substitution of the expansion, Eq. (5) including $\eta(\vec{r}_{ij})$, and projection on the PH for the (ij) partition gives

$$\left[-\frac{\hbar^2}{m}\frac{d^2}{dr^2} + \frac{\hbar^2}{mr^2}\{\mathcal{L}(\mathcal{L}+1) + 4K(K+\alpha+\beta+1)\} + V_{\text{trap}}(r) - E_R\right]U_{Kl}(r) + \sum_{K'} f_{Kl}V_{KK'}(r)f_{K'l}U_{K'l}(r) = 0, \tag{9}$$

where $U_{Kl}(r) = f_{Kl}\ u^l_K(r)$, $\mathcal{L} = l + \frac{3N-6}{2}$, $\alpha = \frac{3N-8}{2}$, $\beta = l + \frac{1}{2}$, l being the orbital angular momentum of the system contributed by the interacting pair. The constant f^2_{Kl} represents the overlap of the PH for interacting partition with the sum of the full set of PH for all partitions and its expression in a closed form can be found in Ref. [29]. The resulting potential matrix element $V_{KK'}(r)$ is given by [24]

$$V_{KK'}(r) = \left(h^{\alpha\beta}_K h^{\alpha\beta}_{K'}\right)^{-\frac{1}{2}} \int_{-1}^{+1} \left\{P^{\alpha\beta}_K(z)V\left(r\sqrt{\frac{1+z}{2}}\right) \times P^{\alpha\beta}_{K'}(z)\eta\left(r\sqrt{\frac{1+z}{2}}\right)W_l(z)\right\}dz, \tag{10}$$

where $h^{\alpha\beta}_K$ and $W_l(z)$ are, respectively, the norm and weight function of the Jacobi polynomial $P^{\alpha\beta}_K(z)$ [31]. Inclusion of the short-range correlation function $\eta(r_{ij})$ makes the PH basis nonorthogonal. Standard procedure for handling a nonorthogonal basis can be followed. However, dependence of the overlap $\langle \mathcal{P}^{lm}_{2K+l}(\Omega^{(ij)}_{N'})\mathcal{P}^{lm}_{2K'+l}(\Omega^{(kl)}_{N'})\eta(r_{kl})\rangle$ on the hyperradius r makes this very involved. On the other hand, actual numerical calculation shows that this overlap matrix is nearly a constant times the unit matrix, except for a small interval of r near r_c. Disregarding its derivatives, we approximately get Eq. (9), with an effective potential matrix element given by Eq. (10). One notices that *the effective two-body interaction seen by the pair* is governed by a_s through $\eta(\vec{r}_{ij})$ and becomes $V(r_{ij})\eta(r_{ij})$. One can understand this physically as follows. Since the interacting atoms in the BEC have very low energy, a pair of them do not come close enough to "see" the *actual* interatomic interaction. (Note that $\eta(r_{ij})$ is vanishingly small for small values of $\vec{r}_{ij}$ [25]).

The procedure of introduction of the PH basis and inclusion of the short-range correlation function, which is collectively referred to as the correlated potential harmonic expansion (CPHE) method, reduces the algebraic and numerical complexities drastically, so much so that the N-body problem simplifies to one involving *only four active degrees of freedom*, the remaining unimportant degrees of freedom for the dilute BEC being "frozen." This permits us to solve the system up to $N = 15\,000$ particles in the condensate. For larger N, the quantity α becomes too large to be handled by the computer, especially for the weight function $W_l(z)$ of the Jacobi polynomial. This CPHE technique has been successfully applied and tested against known results, both experimental and theoretical calculated by other authors, for $T = 0$ properties of both repulsive and attractive condensates [23,24,32].

To solve Eq. (9) we adopt the hyperspherical adiabatic approximation (HAA) [33], which not only simplifies the computational complexities, but also it provides an effective potential in the hyperradial space in which the condensate moves. In this approximation, the hyperradial motion is adiabatically separated from the hyperangular motion, assuming the former is much slower than the latter. This assumption is justified, since the hyperradial motion corresponds to the breathing mode. The hyperangular motion is solved by diagonalizing the potential matrix, together with the hypercentrifugal repulsion for a fixed value of r. The lowest eigenvalue, called the lowest eigenpotential $\omega_0(r)$, is used in the adiabatically separated single hyperradial differential equation

$$\left[-\frac{\hbar^2}{m}\frac{d^2}{dr^2} + \omega_0(r) - E_R\right]\zeta_0(r) = 0, \tag{11}$$

to obtain E_R and the hyperradial wave function $\zeta_0(r)$ in the extreme adiabatic approximation (EAA) [33]. We solve Eq. (11) by the Runge-Kutta method, subject to appropriate boundary conditions to get E_R and $\zeta_0(r)$. The center-of-mass energy 1.5 $\hbar\omega$ is added to each energy eigenvalue to obtain the total energy of the system. Orbital angular momentum (l) is a good quantum number for a spherically symmetric trap and central interatomic potential. With $l = 0$, we obtain $E_{n0}, (n = 0,1,2,\ldots)$. In a similar fashion energy levels for $l > 0$ can be calculated as hyperradial excitations in the effective eigenpotential corresponding to a particular l. However, there are serious numerical problems arising from the fact that the weight function $W_l(z)$ becomes very critical for $l > 0$, so that numerical evaluation of Eq. (10) involves a large error. Hence we take the potential matrix element for $l = 0$ (which does not change much with l) and add the hypercentrifugal term corresponding to the chosen value of l. In incorporating the hypercentrifugal term, the shift of minimum value of the hyperradius corresponding to $\omega_0(r)$ is taken into account and approximated so as to yield the correct contribution of the centrifugal term.

Before closing the discussion we must say that the theoretical formulation used in this manuscript (CPHE) to calculate

several statistical fluctuations of Bose-Einstein condensate accurately describes the correlation in bosonic systems and goes beyond the mean-field approximation. The system which is considered in the present work mimics the BEC of the JILA trap, which is dilute. In this typical experiment as the density of the Bose gas is small, only interactions between two particles at a time are expected to play a major role. To make the problem manageable, we restrict the basis by allowing only two-body correlations, which is vital for the experimental condensate. However, for dense systems the effect of higher-body correlations may come into the picture. The present formalism is applicable for short-range and attractive interaction. It can also successfully consider the realistic van der Waals potential with a short-range hard core and long-range tail, which allows us to observe the effect of long-range interaction in the calculation of several condensate properties. The success is spectacular for attractive BEC where the inclusion of two-body correlation makes a drastic difference in the calculation of critical coefficient defined as $N_{cr}a_s/a_{ho}$ with the mean-field results [25]. As the correlated basis set keeps all two-body correlations, the effective degrees of freedom is always four, which makes the calculation manageable even for quite a large number of bosons [32]. It also allows us to study the finite-size effect over the mean field when the number of bosons is truly finite in the experimental BEC. The calculation of low-lying collective excitations and their comparison with mean-field results is also reported [32]. Several thermodynamic properties, including the specific heat, condensation temperature, and condensate fraction, have been recently calculated for the same system and their comparison with the experimental and mean-field results was also reported recently [32]. Thus the CPHE basis is a very effective basis for the consideration of experimental BEC of the JILA trap and gives generic features. We believe also that the use of a two-body correlated basis function for an exhaustive study of the statistical fluctuation will calculate fluctuation measures accurately. Although currently there are no reported experimental results, we believe that our theoretical results may be important for future experiments.

III. RESULTS

A. Canonical recursion relation for weakly interacting gas

As noted earlier, for the present study we start from the canonical ensemble, which considers the intermediate situation of the microcanonical ensemble and the grand-canonical ensemble. In the microcanonical ensemble the gas is completely isolated and there is no exchange of energy or atoms, whereas in the grand-canonical ensemble, only the average energy per atom and the average number of atoms are fixed; thus there is an exchange of both energy and atoms which leads to the grand-canonical catastrophe [6]. Thus we restrict our discussion to the canonical ensemble, which is the most appealing approach.

Long ago Landsberg proposed a recursion method for calculation of the partition function of the canonical ensemble using iteration technique. Thus the partition function Z_n of a canonical ensemble can be calculated by a simple algorithm [7,26] as

$$Z_n = \frac{1}{n}\sum_{p=1}^{n} S_p Z_{n-p}, \quad Z_0 = 1, \quad \text{and} \quad n = 1,2,...,N, \tag{12}$$

where,

$$S_p = \sum_j \exp\left(\frac{pE_j}{k_B T}\right). \tag{13}$$

In the present case, it is given by

$$S_p = \sum_{n=0}^{\infty}\sum_{l=0}^{\infty}(2l+1)\exp\left(\frac{E_{nl}}{k_B T}\right), \tag{14}$$

where E_{nl} corresponds to the energy level with n and l quantum numbers. As mentioned earlier, the energy levels are calculated in the lowest eigenpotential $\omega_0(r)$ which is obtained by solving the adiabatically separated hyperradial differential equation. Thus in our methodology the problem of N-correlated bosons is simply reduced to an effective one-dimensional problem in the hyperradial space. The whole condensate moves as a single quantum stuff in the ω_0. Thus further using $\omega_0(r)$, one can in principle get all the physical insight of the condensate properties. Our calculated ground-state energy and low-lying collective excitations are in good agreement with the experimental results. The results are compared with mean-field and hydrodynamic results [32]. The beyond mean-field effect is discussed. Thus although we solve the effective one-body potential for the calculation of ground and several low-lying and high-lying excitations, the effect of correlation inherently comes through the calculation of $\omega_0(r)$. The effect of correlation and correlation energy are also discussed in our earlier issues. Thus the calculation of energy levels which are further used for the calculation of the partition function retains the effect of correlation and can be used for the calculation of fluctuation near and above T_c.

In our numerical procedure, we calculate a large number of energy levels E_{nl} with n and l running typically from 0 to 300 and 0 to 200, respectively. The upper cutoff in n and l are finally determined by the convergence in the chemical potential [34].

These relations above are generally used to calculate the partition function for a moderate number of particles ($N < 1000$). For a larger number of particles accuracy drops drastically due to the inability of handling large numbers by the computer. To overcome this computational difficulty, another method [26] is used, where at each step of iteration the partition function is normalized. The relevant relations are

$$Z_0^{\{0\}} = 1, \tag{15}$$

$$Z_n^{\{n-1\}} = \sum_{p=0}^{n-1}\frac{S_{n-p}Z_p^{\{n-1\}}}{n}, \quad n = 1,.....,N, \tag{16}$$

$$Z_k^{\{n\}} = \frac{Z_k^{\{n-1\}}}{\sum_{p=0}^{n} Z_p^{\{n-1\}}}, \quad k = 0,.....,n. \tag{17}$$

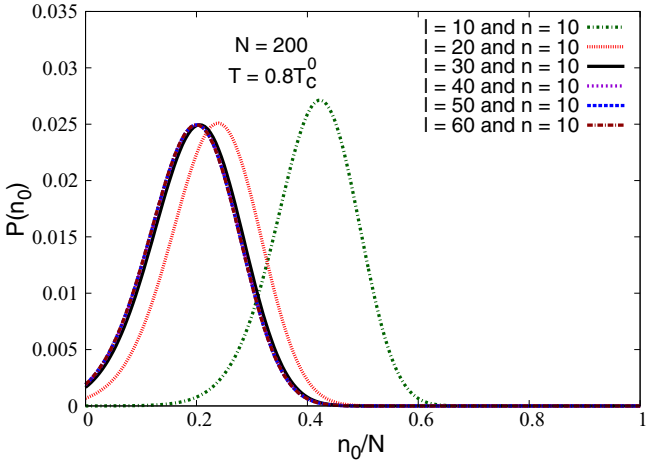

FIG. 1. Plot of ground-state probability $P(n_0)$ against n_0/N for noninteracting bosons with $N = 200$ in the harmonic trap at $T = 0.8T_c^0$ for various l values. In this case n is kept fixed and convergence is shown for different l values. A similar convergence can also established by varying n and keeping l fixed.

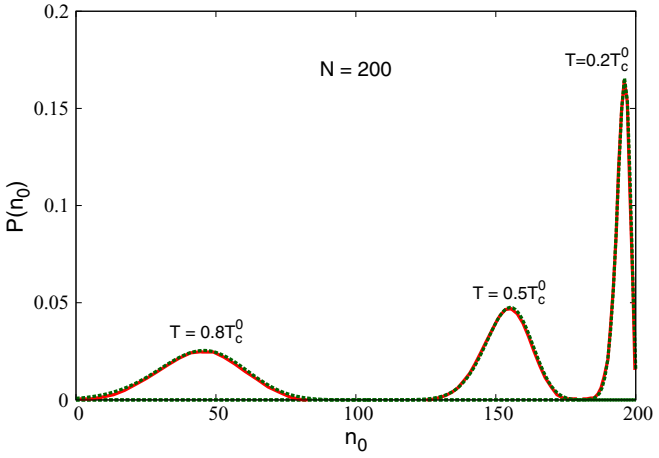

FIG. 2. Plot of ground-state probability $P(n_0)$ against n_0 for noninteracting bosons with $N = 200$ in the harmonic trap at different temperatures calculated by PHEM (dotted green lines). The curves with the solid (red) lines correspond to results obtained from the canonical ensemble quasiparticle techniques [18].

The probability to find n particles in the ground state is

$$P_n^{(0)} = Z_{N-n}^{\{N\}}, \tag{18}$$

$$Z_N = Z_N^{\{n\}} \Pi_{n=1}^{N} \sum_{p=0}^{n} Z_p^{\{n-1\}}. \tag{19}$$

The general relation between the probability distribution of the n_0 number of atoms in the ground state (P_{n_0}) and the canonical partition function is

$$P_{n_0} = \frac{Z_{N-n_0}(T) - Z_{N-n_0-1}(T)}{Z_N(T)}. \tag{20}$$

The average number of atoms in the ground state of the trap is then defined as

$$\langle n_0 \rangle = \sum_{n_0=0}^{N} n_0 P_{n_0}. \tag{21}$$

The central moments are then obtained as

$$\langle (n_0 - \bar{n}_0)^m \rangle = \sum_{n_0=0}^{N} (n_0 - \bar{n_0})^m P_{n_0}. \tag{22}$$

B. Ideal Bose gas under harmonic confinement

We consider the dilute gas of Bose atoms when the interatomic scattering length is neglected. The gas is confined inside a trap so that the number of atoms N is fixed. For the calculation of E_{nl} for $l > 0$ we follow our earlier trick [34,35] and look for the convergence in the probability distribution for fixed temperature. In Fig. 1 we plot the probability distribution $P(n_0)$ for $N = 200$ noninteracting bosons at $T = 0.8T_c$ for various choices of n and l, which exhibit nice convergence.

The recursion relations described above are used to determine the probability distribution of the condensate at a particular temperature. In Fig. 2, we plot the distribution of the atom number in the ground state of the trap for $N = 200$ atoms at $T = 0.2T_c, 0.5T_c, 0.8T_c$.

For the ideal gas one can have the exact probability distribution of the number of uncondensed atoms. In Fig. 2, we observe that with an increase in temperature, the condensate in the ground state is depleted as the probability of uncondensed atoms in the higher states gradually increases. Thus the peak value of P_{n_0} decreases with increase in T. At $T \ll T_c$, the distribution shows a sharp peak near $\bar{n}_0$ and becomes broader at higher T. Condensation of N bosons has also been studied by some effective formulations earlier. One uses a master equation together with a canonical ensemble of quasiparticle techniques [18]. Upon comparison of our numerical simulation with Fig. 2 of Ref. [18], we observe excellent agreement at all temperatures.

Next we calculate the average condensate particle number $\langle n_0 \rangle$, its variance $\triangle n_0$, the third central moment $\langle (n_0 - \bar{n}_0)^3 \rangle$, and the fourth central moment $\langle (n_0 - \bar{n}_0)^4 \rangle$.

We plot them in Fig. 3 for an ideal gas of $N = 200$ particles in a harmonic trap. For comparison with earlier calculations (CNB5) [18], we plot the results of CNB5 as the dots. The nice agreement with our numerical results for the ideal gas proves the accuracy of our numerical many-body computation.

C. Interacting Bose gas under harmonic confinement

Although the earlier calculation of IG Bose gas has been extended to consider the interacting bosons [21,36], we do not find any research work which considers the realistic situation where N interacting atoms are in the external harmonic trap. All previous papers in this area dealt with N atoms confined in a rectangular box with periodic boundary conditions. It is already pointed out that in such a box confinement with periodic boundary conditions the condensate will still have the zero-momentum component of the atomic field which corresponds to the ideal gas. Next, in the Bogoliubov quasiparticle excitation spectrum, the quasiparticles are treated as independent bosons. Thus none of these papers fully take

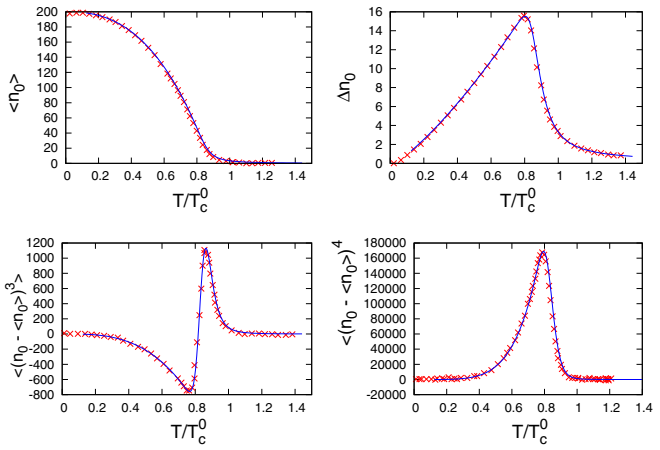

FIG. 3. Plot of different moments against T/T_c^0 for $N = 200$ in the harmonic trap by PHEM (blue solid lines) and comparison with the result obtained from the canonical ensemble quasiparticle techniques (red points) [18].

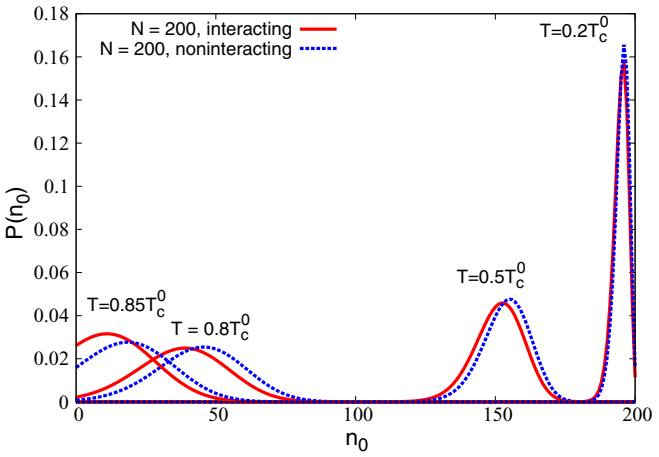

FIG. 4. Plot of ground-state probability $P(n_0)$ against n_0 for interacting bosons with $N = 200$ in the harmonic trap at different temperatures calculated by PHEM (solid red lines). The curves with the dotted (blue) lines correspond to the noninteracting bosons.

into account the interacting Hamiltonian. Thus the main motivation of our present work is to push our quantum many-body calculation to the real experimental situation where we truly consider the effect of the interacting Hamiltonian. We consider a finite number of atoms, which allows us to study the mesoscopic regime. We calculate several fluctuation measures for the interacting gas in the harmonic trap and observe the effect of repulsive interaction on the ground-state distribution and the statistical behavior of the N-atom condensate. We choose the spherically symmetric trap of frequency 77.78 Hz as the external trap which mimics the JILA experiment with ^{87}Rb atoms. The parameters of the van der Waals interaction are chosen, which accurately describes the Rb–Rb interaction and corresponds to the scattering length of 100 Bohr, which directly relates the JILA experiment for the interacting BEC.

We perform the following calculation for an N-atom trapped system where the dimer interaction is represented by the scattering length $a_s = 0.004\,33$ o.u., which corresponds to the Rb condensate in the JILA trap [5]. The external trap remains the same as used for the calculation of ideal Bose gas. In Fig. 4, we plot the results of P_{n_0} as a function of n_0 for particle number as $N = 200$. The effective interaction of the condensate is defined by the quantity Na_s, which is repulsive for the present choices of N and a_s.

From Fig. 4 we observe that the repulsive interaction among the atoms reduces the distribution significantly. This implies that the repulsive interaction enhances the population in the excited states with appropriate depletion in the ground state.

In Fig. 5(a), we present the condensate fraction as a function of temperature for different interaction strengths $na_s^{1/3} = 0.02$, 0.03, 0433 which correspond to $N = 100$, 500, 1000 atoms under confinement when the ideal Bose gas corresponds to $na_s^{1/3} = 0$. We observe that the condensate fraction exhibits a smooth transition while passing the critical temperature. It nicely shows that the repulsive interaction reduces the mean condensate occupation in the ground state.

In Figs. 5(b)–5(d) we plot several fluctuation quantities such as the second, third, and fourth central moments of the condensate for the same interaction parameters used to define the mean occupation of the condensate. All the observations made in Figs. 5(a)–5(d) are consistent with each other.

In order to study the temperature dependence of fluctuations, the standard deviations (σ) have been plotted in Fig. 6, against the temperature $\frac{k_B T}{\hbar\omega}$. The curves exhibit a maximum at a particular temperature and then drop to zero. It is interesting to note that at low temperature the fluctuations are independent of the total particle number (N) and this independence persists up to the critical temperature. Beyond the critical temperature the fluctuations go to zero, as expected.

Next we take the opportunity to define the mesoscopic effect in BEC and to define the critical temperature. In recent experiments of BEC in ultracold gases, the number of condensed atoms is truly finite, and as $N \simeq 10^2$–10^3, the condensate is mesoscopic rather than macroscopic. Thus it is interesting to analyze further mesoscopic effect associated with the calculation of fluctuation in the interacting Bose gas. At high temperature ($T > T_c$), the average number of atoms in the ground state is finite for the finite-size condensate. But below the critical temperature ($T < T_c$), the occupation in the ground state of the trap is macroscopically large, which is nicely reflected in our calculation. In Figs. 5(a)–5(d), we explicitly demonstrate a smooth transition for a mesoscopic regime ($\simeq$100 atoms) to quite a large system containing a few thousands of atoms. At the threshold point ($T = T_c$), the fluctuation changes sharply for a large particle limit from which one may consider the possibility of phase transition at the critical temperature for a large N limit. However, for systems containing a few hundred atoms, there is not a sharp critical point. Here we define a critical characteristic value of temperature where the standard deviation sharply drops to zero in Fig. 6, where we plot the standard deviation as a function of $\frac{k_B T}{\hbar\omega}$. In Table I, we present the values of critical temperature for various numbers of atoms in the trap.

D. Thermodynamics of mesoscopic BEC

The thermodynamics of mesoscopic BEC has been studied before incorporating the correction to the thermodynamic

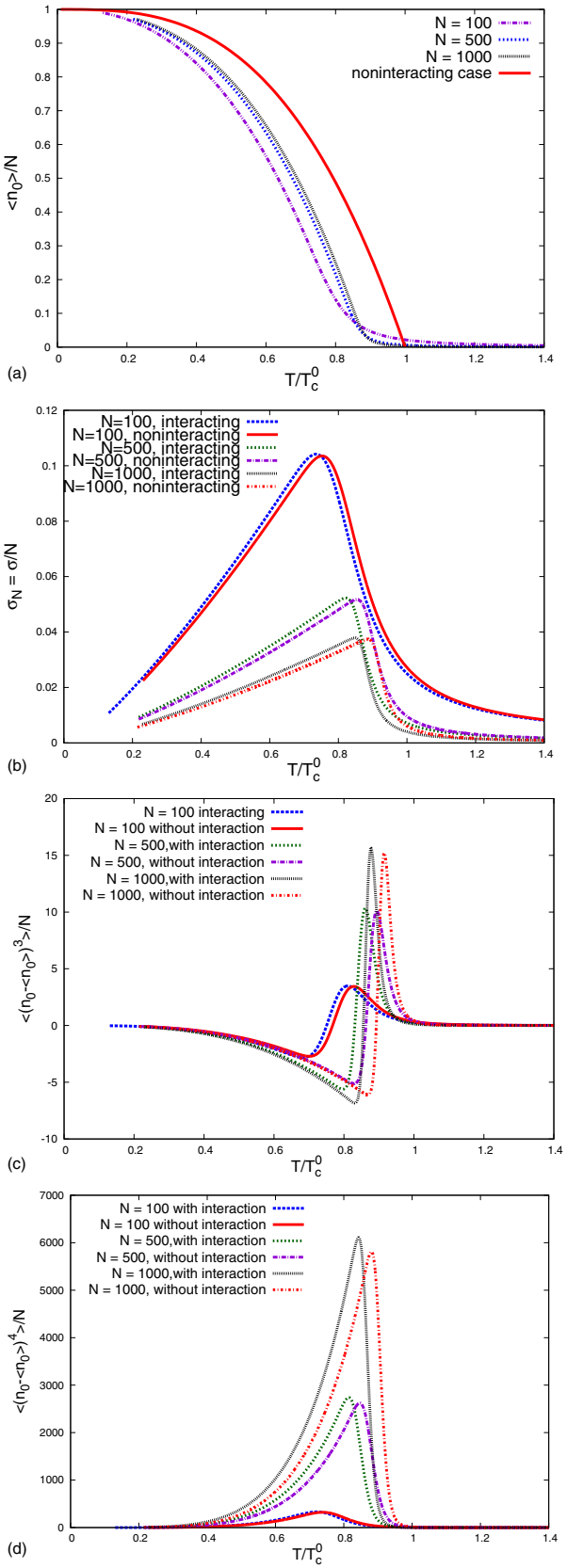

FIG. 5. Plot of condensate fraction n_0/N [panel (a)], standard deviation [panel (b)], 3rd moment [panel (c)], and 4th moment [panel (d)] against the reduced temperature T/T_c^0 for indicated numbers of interacting bosons in the harmonic trap.

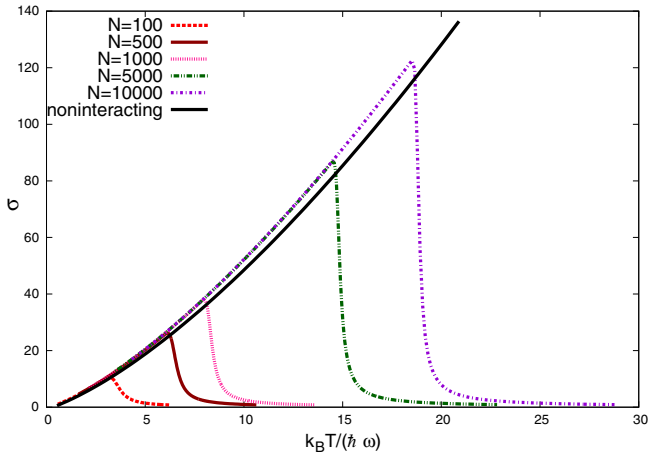

FIG. 6. Plot of the standard deviation against $\frac{k_B T}{\hbar\omega}$ for indicated number of interacting bosons in the harmonic trap. The black (solid) curve displays the result [12] with the noninteracting particles.

quantities due to the finite number of particles and weak interaction [9]. The finite particle number constraint gives the additive correction to the thermodynamic quantities in the critical region [21,37–39]. However, our calculated many-body approach takes care of the effect of a finite-sized system already. Thus in our approach the thermodynamic quantities are directly calculated from the Bose distribution function

$$f(E_{nl}) = \frac{1}{e^{\beta(E_{nl}-\mu)} - 1} \tag{23}$$

and μ is the chemical potential obtained from

$$N = \sum_{n=0}^{\infty}\sum_{l=0}^{\infty}(2l+1)f(E_{nl}). \tag{24}$$

At $T = 0$, μ is equal to the ground-state energy, where all the bosons occupy this level. The total energy of the condensate at temperature T is calculated from

$$\langle E(N,T)\rangle = \sum_{n=0}^{\infty}\sum_{l=0}^{\infty} E_{nl}P(E_{nl}) = \sum_{n=0}^{\infty}\sum_{l=0}^{\infty}\frac{(2l+1)f(E_{nl})E_{nl}}{N}. \tag{25}$$

The specific heat of the condensate for a fixed particle number is calculated as

$$C_A(T) = \left.\frac{\partial E(A,T)}{\partial T}\right|_A. \tag{26}$$

TABLE I. Critical temperatures of the condensate for different particle numbers (A).

A	T_c^0 (nK)	T_c/T_c^0
50	12.934	0.691
100	16.295	0.735
200	20.531	0.784
500	27.865	0.820
1000	35.108	0.848

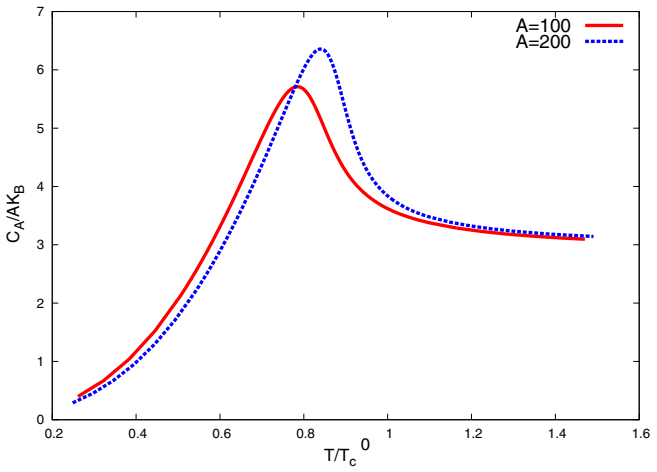

FIG. 7. Plot of $(\frac{C_A}{Ak_B})$ as a function of $\frac{T}{T_c^0}$ for WIG with $A = 100$ and 200 particles in the harmonic trap.

For a truly mesoscopic region, as $C_A(T)$ changes smoothly(exhibiting a hump at $T = T_c$), it is not possible to define the critical temperature and we are also not able to provide an analytic expression for T_c. However, we can define a transition temperature T_c at which $C_A(T)$ exhibits the maximum. Thus $\frac{\partial C_A(T)}{\partial T}|_{T=T_C} = 0$. Heat capacity per particle $(\frac{C_A}{Nk_B})$ as a function of T for WIG with $N=$ 100 and 200 particles is shown in Fig. 7, where T_c^0 is the thermodynamic temperature defined by [30]

$$T_c^0 = \left[\frac{A}{\zeta(3)}\right]^{1/3} \frac{\hbar\omega}{k}. \tag{27}$$

It can be noticed that for $T \gg T_c$, the heat capacity is equal to the thermodynamic value of an ideal gas with $C_A = \frac{3}{2}N$. At higher T, the atoms behave classically. For low temperature the interaction effect is prominent. It is to be noted that interaction substantially increases the heat capacity in the critical region and sharpens the peak.

Finally, the critical temperature of the condensate for different particle numbers (A) in the mesoscopic regime is presented in Table I. T_c^0 is the critical temperature in the thermodynamic limit defined through Eq. (27) and T_c is the critical temperature of the condensate with interaction obtained from the maximum of the standard deviation curves calculated by CPHE method.

IV. CONCLUSION

In this paper we calculate several condensate statistics for the interacting Bose gas in the harmonic confinement for various interaction strengths and in the framework of correlated many-body formalism. The method by which we calculate the energy spectrum basically keeps all possible two-body correlations and uses van der Waals interaction. Although the condensation of N interacting bosons has been studied earlier, none of them has considered the real experimental situation. We considered the BEC in the JILA trap and studied the interacting bosons in harmonic confinement. The use of a correlated basis function and van der Waals interaction exhibits the generic features. Our results for ideal gas are in good agreement with the earlier calculation, which exhibits the accuracy of our numerical results. We also calculate the various fluctuations near the critical points and observe the effect of interaction. We also study the mesoscopic BEC where the number of bosons is truly finite and is of great interest in present day experiments.

As mentioned earlier, the calculation of fluctuations of a finite number of interacting condensate particles is rather delicate and requires accurate description. We also addressed several published papers which deal with various limiting cases. However, here we present a complete many-body calculation including interatomic correlation and using realistic van der Waals interaction. Our method considers very few to a quite large number of systems and offers thorough investigation of a truly mesoscopic system near and above T_c. Instead of box confinement we consider the real experimental scenario where the atoms are trapped under harmonic confinement. The calculated several fluctuation properties are qualitatively the same as those obtained for box confinement. However, the comparison of quantitative agreement or disagreement between these two is not possible, as the choice of interaction and the nature of confinement is different. The box confinement is rather a model calculation, whereas our calculation considers a real experimental situation. Although the BEC is often considered as an atom laser and the study of BEC statistics near T_c is analogous to the study of photon statistics, we do not find any experimental results which directly support our results for the moment. However, our theoretical results may be verified for future experiments.

ACKNOWLEDGMENTS

The authors wish to thank Prof. T. K. Das of University of Calcutta, India, for useful discussion. S.B. acknowledges the support of University Grants Commission, India, for a Major Research Project [F. No. 40-439/2011(SR)] and the present work is a part of this project. B.C. would like to acknowledge the financial support of the DST (Government of India) through Contract No. SR/S2/CMP/0126/2012.

[1] M. H. Anderson, J. R. Ensher, M. R. Matthews, C. E. Wieman, and E. A. Cornell, Science **269**, 198 (1995).
[2] C. C. Bradley, C. A. Sackett, J. J. Tollett, and R. G. Hulet, Phys. Rev. Lett. **75**, 1687 (1995).
[3] K. B. Davis, M. O. Mewes, M. R. Andrews, N. J. vanDruten, D. S. Durfee, D. M. Kurn, and W. Ketterle, Phys. Rev. Lett. **75**, 3969 (1995).
[4] J. R. Ensher, D. S. Jin, M. R. Matthews, C. E. Wieman, and E. A. Cornell, Phys. Rev. Lett. **77**, 4984 (1996).
[5] S. L. Cornish, N. R. Claussen, J. L. Roberts, E. A. Cornell, and C. E. Wieman, Phys. Rev. Lett. **85**, 1795 (2000).
[6] N. L. Balazs and T. Bergeman, Phys. Rev. A **58**, 2359 (1998).

[7] T. Landsberg, *Thermodynamics with Qunatum Statistical Illustration* (Interscience, New York, 1961); K. Kirsten and D. J. Toms, Phys. Rev. A **54**, 4188 (1996).

[8] K. Glaum, H. Kleinert, and A. Pelster, Phys. Rev. A **76**, 063604 (2007).

[9] V. V. Kocharovsky *et al.*, Adv. At. Mol. Opt. Phys. **53**, 291 (2006); V. V. Kocharovsky, M. O. Scully, S. Y. Zhu, and M. S. Zubairy, Phys. Rev. A **61**, 023609 (2000).

[10] L. Pitaevskii and S. Stringari, *Bose-Einstein Condensation* (Oxford University Press, Oxford, UK, 2003).

[11] S. Grossmann and M. Holthaus, Phys. Rev. Lett. **79**, 3557 (1997).

[12] M. Holthaus and E. Kalinowski, Ann. Phys. (NY) **276**, 321 (1999).

[13] P. Navez, D. Bitouk, M. Gajda, Z. Idziaszek, and K. Rzazewski, Phys. Rev. Lett. **79**, 1789 (1997).

[14] S. Giorgini, L. P. Pitaevskii, and S. Stringari, Phys. Rev. Lett. **80**, 5040 (1998).

[15] H. Xiong, S. Liu, G. Huang, and Z. Xu, Phys. Rev. A **65**, 033609 (2002).

[16] V. V. Kocharovsky and Vl. V. Kocharovsky, Phys. Rev. A **81**, 033615 (2010).

[17] V. V. Kocharovsky, Vl. V. Kocharovsky, and M. O. Scully, Phys. Rev. Lett. **84**, 2306 (2000).

[18] A. A. Svidzinsky and M. O. Scully, Phys. Rev. Lett. **97**, 190402 (2006).

[19] Idziaszek *et al.*, Europhys. Lett. **86**, 10002 (2009).

[20] J. Wang and J. He, Phys. Rev. E **83**, 051132 (2011).

[21] K. E. Dorfman, M. Kim, and A. A. Svidzinsky, Phys. Rev. A **83**, 033609 (2011).

[22] A. Svidzinsky and M. Scully, Phys. Rev. A **82**, 063630 (2010).

[23] T. K. Das and B. Chakrabarti, Phys. Rev. A **70**, 063601 (2004).

[24] T. K. Das, S. Canuto, A. Kundu, and B. Chakrabarti, Phys. Rev. A **75**, 042705 (2007).

[25] T. K. Das, A. Kundu, S. Canuto, and B. Chakrabarti, Phys. Lett. A **373**, 258 (2009).

[26] E. D. Trifonov and S. N. Zagoulaev, Phys.-Usp. **53**, 83 (2010).

[27] J. L. Ballot and M. Fabre de la Ripelle, Ann. Phys. (NY) **127**, 62 (1980).

[28] M. Gattobigio and A. Kievsky, Phys. Rev. A **90**, 012502 (2014).

[29] M. Fabre de la Ripelle, Ann. Phys. (NY) **147**, 281 (1983).

[30] C. J. Pethick and H. Smith, *Bose-Einstein Condensation in Dilute Gases* (Cambridge University Press, Cambridge, UK, 2002).

[31] M. Abramowitz and I. A. Stegun, *Handbook of Mathematical Functions* (National Institute of Standards and Technology, Gaithersburg, MD, 1964).

[32] M. L. Lekala, B. Chakrabarti, G. J. Rampho, T. K. Das, S. A. Sofianos, and R. M. Adam, Phys. Rev. A **89**, 023624 (2014); S. A. Sofianos, T. K. Das, B. Chakrabarti, M. L. Lekala, R. M. Adam, and G. J. Rampho, *ibid.* **87**, 013608 (2013); B. Chakrabarti, T. K. Das, and P. K. Debnath, *ibid.* **79**, 053629 (2009); A. Biswas, B. Chakrabarti, and T. K. Das, J. Chem. Phys. **133**, 104502 (2010); S. K. Haldar, B. Chakrabarti, and T. K. Das, Phys. Rev. A **82**, 043616 (2010); A. Biswas, T. K. Das, L. Salasnich, and B. Chakrabarti, *ibid.* **82**, 043607 (2010); P. K. Debnath and B. Chakrabarti, *ibid.* **82**, 043614 (2010); A. Biswas, B. Chakrabarti, T. K. Das, and L. Salasnich, *ibid.* **84**, 043631 (2011); A. Biswas, J. Phys. B **42**, 215302 (2009).

[33] T. K. Das, H. T. Coelho, and M. Fabre de la Ripelle, Phys. Rev. C **26**, 2281 (1982).

[34] S. Bhattacharyya, T. K. Das, and B. Chakrabarti, Phys. Rev. A **88**, 053614 (2013).

[35] S. Goswami, T. K. Das, and A. Biswas, Phys. Rev. A **84**, 053617 (2011).

[36] J. H. Wang, H. Y. Tang, and Y. L. Ma, Ann. Phys. (NY) **326**, 634 (2011).

[37] J.-H. Wang and Y.-L. Ma, Phys. Rev. A **79**, 033604 (2009).

[38] C. C. Bradley, C. A. Sackett, and R. G. Hulet, Phys. Rev. Lett. **78**, 985 (1997).

[39] D. J. Han, R. H. Wynar, Ph. Courteille, and D. J. Heinzen, Phys. Rev. A **57**, R4114(R) (1998); U. Ernst, A. Marte, F. Schreck, J. Schuster, and G. Rempe, Europhys. Lett. **41**, 1 (1998); L. V. Hau, B. D. Busch, C. Liu, Z. Dutton, M. M. Burns, and J. A. Golovchenko, Phys. Rev. A **58**, R54 (1998).